

Search for invisible decays of a dark photon using e^+e^- annihilation data at BESIII

M. Ablikim¹, M. N. Achasov^{11,b}, P. Adlarson⁷⁰, M. Albrecht⁴, R. Aliberti³¹, A. Amoroso^{69A,69C}, M. R. An³⁵, Q. An^{66,53}, X. H. Bai⁶¹, Y. Bai⁵², O. Bakina³², R. Baldini Ferroli^{26A}, I. Balossino^{27A}, Y. Ban^{42,g}, V. Batzskaya^{1,40}, D. Becker³¹, K. Begzsuren²⁹, N. Berger³¹, M. Bertani^{26A}, D. Bettoni^{27A}, F. Bianchi^{69A,69C}, J. Bloms⁶³, A. Bortone^{69A,69C}, I. Boyko³², R. A. Briere⁵, A. Brueggemann⁶³, H. Cai⁷¹, X. Cai^{1,53}, A. Calcaterra^{26A}, G. F. Cao^{1,58}, N. Cao^{1,58}, S. A. Cetin^{57A}, J. F. Chang^{1,53}, W. L. Chang^{1,58}, G. Chelkov^{32,a}, C. Chen³⁹, Chao Chen⁵⁰, G. Chen¹, H. S. Chen^{1,58}, M. L. Chen^{1,53,58}, S. J. Chen³⁸, S. M. Chen⁵⁶, T. Chen^{1,58}, X. R. Chen^{28,58}, X. T. Chen^{1,58}, Y. B. Chen^{1,53}, Z. J. Chen^{23,h}, W. S. Cheng^{69C}, S. K. Choi⁵⁰, X. Chu³⁹, G. Cibinetto^{27A}, S. C. Coen⁴, F. Cossio^{69C}, J. J. Cui⁴⁵, H. L. Dai^{1,53}, J. P. Dai⁷³, A. Dbeyssi¹⁷, R. E. de Boer⁴, D. Dedovich³², Z. Y. Deng¹, A. Denig³¹, I. Denysenko³², M. Destefanis^{69A,69C}, F. De Mori^{69A,69C}, Y. Ding³⁶, J. Dong^{1,53}, L. Y. Dong^{1,58}, M. Y. Dong^{1,53,58}, X. Dong⁷¹, S. X. Du⁷⁵, P. Egorov^{32,a}, Y. L. Fan⁷¹, J. Fang^{1,53}, S. S. Fang^{1,58}, W. X. Fang¹, Y. Fang¹, R. Farinelli^{27A}, L. Fava^{69B,69C}, F. Feldbauer⁴, G. Felici^{26A}, C. Q. Feng^{66,53}, J. H. Feng⁵⁴, J. H. Fischer⁶⁴, M. Fritsch⁴, C. Fritzsche⁶³, C. D. Fu¹, H. Gao⁵⁸, Y. N. Gao^{42,g}, Yang Gao^{66,53}, S. Garbolino^{69C}, I. Garzia^{27A,27B}, P. T. Ge⁷¹, Z. W. Ge³⁸, C. Geng⁵⁴, E. M. Gersabeck⁶², A. Gilman⁶⁴, K. Goetzen¹², L. Gong³⁶, W. X. Gong^{1,53}, W. Gradl³¹, M. Greco^{69A,69C}, L. M. Gu³⁸, M. H. Gu^{1,53}, Y. T. Gu¹⁴, C. Y. Guan^{1,58}, A. Q. Guo^{28,58}, L. B. Guo³⁷, R. P. Guo⁴⁴, Y. P. Guo^{10,f}, A. Guskov^{32,a}, T. T. Han⁴⁵, W. Y. Han³⁵, X. Q. Hao¹⁸, F. A. Harris⁶⁰, K. K. He⁵⁰, K. L. He^{1,58}, F. H. Heinsius⁴, C. H. Heinz³¹, Y. K. Heng^{1,53,58}, C. Herold⁵⁵, M. Himmelreich^{31,d}, T. Holtmann⁴, G. Y. Hou^{1,58}, Y. R. Hou⁵⁸, Z. L. Hou¹, H. M. Hu^{1,58}, J. F. Hu^{51,i}, T. Hu^{1,53,58}, Y. Hu¹, G. S. Huang^{66,53}, K. X. Huang⁵⁴, L. Q. Huang^{28,58}, L. Q. Huang⁶⁷, X. T. Huang⁴⁵, Y. P. Huang¹, T. Hussain⁶⁸, N. Hüskens^{25,31}, W. Imoehl²⁵, M. Irshad^{66,53}, J. Jackson²⁵, S. Jaeger⁴, S. Janchiv²⁹, E. Jang⁵⁰, J. H. Jeong⁵⁰, Q. Ji¹, Q. P. Ji¹⁸, X. B. Ji^{1,58}, X. L. Ji^{1,53}, Y. Y. Ji⁴⁵, Z. K. Jia^{66,53}, H. B. Jiang⁴⁵, S. S. Jiang³⁵, X. S. Jiang^{1,53,58}, Y. Jiang⁵⁸, J. B. Jiao⁴⁵, Z. Jiao²¹, S. Jin³⁸, Y. Jin⁶¹, M. Q. Jing^{1,58}, T. Johansson⁷⁰, N. Kalantar-Nayestanaki⁵⁹, X. S. Kang³⁶, R. Kappert⁵⁹, M. Kavatsyuk⁵⁹, B. C. Ke⁷⁵, I. K. Keshk⁴, A. Khoukaz⁶³, R. Kiuchi¹, R. Kliemt¹², L. Koch³³, O. B. Kolcu^{57A}, B. Kopf⁴, M. Kuemmel⁴, M. Kuessner⁴, A. Kupsc^{40,70}, W. Kühn³³, J. J. Lane⁶², J. S. Lange³³, P. Larin¹⁷, A. Lavania²⁴, L. Lavezzi^{69A,69C}, T. T. Lei^{66,k}, Z. H. Lei^{66,53}, H. Leithoff³¹, M. Lellmann³¹, T. Lenz³¹, C. Li³⁹, C. Li⁴³, C. H. Li³⁵, Cheng Li^{66,53}, D. M. Li⁷⁵, F. Li^{1,53}, G. Li¹, H. Li^{66,53}, H. B. Li^{1,58}, H. J. Li¹⁸, H. N. Li^{51,i}, J. Q. Li⁴, J. S. Li⁵⁴, J. W. Li⁴⁵, Ke Li¹, L. J Li^{1,58}, L. K. Li¹, Lei Li³, M. H. Li³⁹, P. R. Li^{34,j,k}, S. X. Li¹⁰, S. Y. Li⁵⁶, T. Li⁴⁵, W. D. Li^{1,58}, W. G. Li¹, X. H. Li^{66,53}, X. L. Li⁴⁵, Xiaoyu Li^{1,58}, Z. X. Li¹⁴, Z. Y. Li⁵⁴, H. Liang^{66,53}, H. Liang^{1,58}, H. Liang³⁰, Y. F. Liang⁴⁹, Y. T. Liang^{28,58}, G. R. Liao¹³, L. Z. Liao⁴⁵, J. Libby²⁴, A. Limphirat⁵⁵, D. X. Lin^{28,58}, T. Lin¹, B. J. Liu¹, C. X. Liu¹, D. Liu^{17,66}, F. H. Liu⁴⁸, Fang Liu¹, Feng Liu⁶, G. M. Liu^{51,i}, H. Liu^{34,j,k}, H. B. Liu¹⁴, H. M. Liu^{1,58}, Huanhuan Liu¹, Huihui Liu¹⁹, J. B. Liu^{66,53}, J. L. Liu⁶⁷, J. Y. Liu^{1,58}, K. Liu¹, K. Y. Liu³⁶, Ke Liu²⁰, L. Liu^{66,53}, Lu Liu³⁹, M. H. Liu^{10,f}, P. L. Liu¹, Q. Liu⁵⁸, S. B. Liu^{66,53}, T. Liu^{10,f}, W. K. Liu³⁹, W. M. Liu^{66,53}, X. Liu^{34,j,k}, Y. Liu^{34,j,k}, Y. B. Liu³⁹, Z. A. Liu^{1,53,58}, Z. Q. Liu⁴⁵, X. C. Lou^{1,53,58}, F. X. Lu⁵⁴, H. J. Lu²¹, J. G. Lu^{1,53}, X. L. Lu¹, Y. Lu⁷, Y. P. Lu^{1,53}, Z. H. Lu^{1,58}, C. L. Luo³⁷, M. X. Luo⁷⁴, T. Luo^{10,f}, X. L. Luo^{1,53}, X. R. Lyu⁵⁸, Y. F. Lyu³⁹, F. C. Ma³⁶, H. L. Ma¹, L. L. Ma⁴⁵, M. M. Ma^{1,58}, Q. M. Ma¹, R. Q. Ma^{1,58}, R. T. Ma⁵⁸, X. Y. Ma^{1,53}, Y. Ma^{42,g}, F. E. Maas¹⁷, M. Maggiora^{69A,69C}, S. Maldaner⁴, S. Malde⁶⁴, A. A. Malik⁶⁸, A. Mangoni^{26B}, Y. J. Mao^{42,g}, Z. P. Mao¹, S. Marcello^{69A,69C}, Z. X. Meng⁶¹, J. G. Messchendorp^{12,59}, G. Mezzadri^{27A}, H. Miao^{1,58}, T. J. Min³⁸, R. E. Mitchell²⁵, X. H. Mo^{1,53,58}, N. Yu. Muchnoi^{11,b}, Y. Nefedov³², F. Nerling^{17,d}, I. B. Nikolaev^{11,b}, Z. Ning^{1,53}, S. Nisar^{9,l}, Y. Niu⁴⁵, S. L. Olsen⁵⁸, Q. Ouyang^{1,53,58}, S. Pacetti^{26B,26C}, X. Pan^{10,f}, Y. Pan⁵², A. Pathak³⁰, Y. P. Pei^{66,53}, M. Pelizaeus⁴, H. P. Peng^{66,53}, K. Peters^{12,d}, J. L. Ping³⁷, R. G. Ping^{1,58}, S. Plura³¹, S. Pogodin³², V. Prasad^{66,53}, F. Z. Qi¹, H. Qi^{66,53}, H. R. Qi⁵⁶, M. Qi³⁸, T. Y. Qi^{10,f}, S. Qian^{1,53}, W. B. Qian⁵⁸, Z. Qian⁵⁴, C. F. Qiao⁵⁸, J. J. Qin⁶⁷, L. Q. Qin¹³, X. P. Qin^{10,f}, X. S. Qin⁴⁵, Z. H. Qin^{1,53}, J. F. Qiu¹, S. Q. Qu⁵⁶, K. H. Rashid⁶⁸, C. F. Redmer³¹, K. J. Ren³⁵, A. Rivetti^{69C}, V. Rodin⁵⁹, M. Rolo^{69C}, G. Rong^{1,58}, Ch. Rosner¹⁷, S. N. Ruan³⁹, A. Sarantsev^{32,c}, Y. Schelhaas³¹, C. Schnier⁴, K. Schoenning⁷⁰, M. Scodeggio^{27A,27B}, K. Y. Shan^{10,f}, W. Shan²², X. Y. Shan^{66,53}, J. F. Shangguan⁵⁰, L. G. Shao^{1,58}, M. Shao^{66,53}, C. P. Shen^{10,f}, H. F. Shen^{1,58}, X. Y. Shen^{1,58}, B. A. Shi⁵⁸, H. C. Shi^{66,53}, J. Y. Shi¹, Q. Q. Shi⁵⁰, R. S. Shi^{1,58}, X. Shi^{1,53}, X. D. Shi^{66,53}, J. J. Song¹⁸, W. M. Song^{30,1}, Y. X. Song^{42,g}, S. Sosio^{69A,69C}, S. Spataro^{69A,69C}, F. Stieler³¹, K. X. Su⁷¹, P. P. Su⁵⁰, Y. J. Su⁵⁸, G. X. Sun¹, H. Sun⁵⁸, H. K. Sun¹, J. F. Sun¹⁸, L. Sun⁷¹, S. S. Sun^{1,58}, T. Sun^{1,58}, W. Y. Sun³⁰, X. Sun^{23,h}, Y. J. Sun^{66,53}, Y. Z. Sun¹, Z. T. Sun⁴⁵, Y. H. Tan⁷¹, Y. X. Tan^{66,53}, C. J. Tang⁴⁹, G. Y. Tang¹, J. Tang⁵⁴, L. Y. Tao⁶⁷, Q. T. Tao^{23,h}, M. Tat⁶⁴, J. X. Teng^{66,53}, V. Thoren⁷⁰, W. H. Tian⁴⁷, Y. Tian^{28,58}, I. Uman^{57B}, B. Wang^{66,53}, B. Wang¹, B. L. Wang⁵⁸, C. W. Wang³⁸, D. Y. Wang^{42,g}, F. Wang⁶⁷, H. J. Wang^{34,j,k}, H. P. Wang^{1,58}, K. Wang^{1,53}, L. L. Wang¹, M. Wang⁴⁵, Meng Wang^{1,58}, S. Wang¹³, S. Wang^{10,f}, T. Wang^{10,f}, T. J. Wang³⁹, W. Wang⁵⁴, W. H. Wang⁷¹, W. P. Wang^{66,53}, X. Wang^{42,g}, X. F. Wang^{34,j,k}, X. L. Wang^{10,f}, Y. Wang⁵⁶, Y. D. Wang⁴¹, Y. F. Wang^{1,53,58}, Y. H. Wang⁴³, Y. Q. Wang¹, Yaqian Wang^{16,1}, Z. Wang^{1,53}, Z. Y. Wang^{1,58}, Ziyi Wang⁵⁸,

D. H. Wei¹³, F. Weidner⁶³, S. P. Wen¹, C. W. Wenzel⁴, D. J. White⁶², U. Wiedner⁴, G. Wilkinson⁶⁴, M. Wolke⁷⁰, L. Wollenberg⁴, J. F. Wu^{1,58}, L. H. Wu¹, L. J. Wu^{1,58}, X. Wu^{10,f}, X. H. Wu³⁰, Y. Wu⁶⁶, Y. J. Wu²⁸, Z. Wu^{1,53}, L. Xia^{66,53}, T. Xiang^{42,g}, D. Xiao^{34,j,k}, G. Y. Xiao³⁸, H. Xiao^{10,f}, S. Y. Xiao¹, Y. L. Xiao^{10,f}, Z. J. Xiao³⁷, C. Xie³⁸, X. H. Xie^{42,g}, Y. Xie⁴⁵, Y. G. Xie^{1,53}, Y. H. Xie⁶, Z. P. Xie^{66,53}, T. Y. Xing^{1,58}, C. F. Xu^{1,58}, C. J. Xu⁵⁴, G. F. Xu¹, H. Y. Xu⁶¹, Q. J. Xu¹⁵, X. P. Xu⁵⁰, Y. C. Xu⁵⁸, Z. P. Xu³⁸, F. Yan^{10,f}, L. Yan^{10,f}, W. B. Yan^{66,53}, W. C. Yan⁷⁵, H. J. Yang^{46,e}, H. L. Yang³⁰, H. X. Yang¹, L. Yang⁴⁷, S. L. Yang⁵⁸, Tao Yang¹, Y. F. Yang³⁹, Y. X. Yang^{1,58}, Yifan Yang^{1,58}, M. Ye^{1,53}, M. H. Ye⁸, J. H. Yin¹, Z. Y. You⁵⁴, B. X. Yu^{1,53,58}, C. X. Yu³⁹, G. Yu^{1,58}, T. Yu⁶⁷, X. D. Yu^{42,g}, C. Z. Yuan^{1,58}, L. Yuan², S. C. Yuan¹, X. Q. Yuan¹, Y. Yuan^{1,58}, Z. Y. Yuan⁵⁴, C. X. Yue³⁵, A. A. Zafar⁶⁸, F. R. Zeng⁴⁵, X. Zeng⁶, Y. Zeng^{23,h}, Y. H. Zhan⁵⁴, A. Q. Zhang^{1,58}, B. L. Zhang^{1,58}, B. X. Zhang¹, D. H. Zhang³⁹, G. Y. Zhang¹⁸, H. Zhang⁶⁶, H. H. Zhang³⁰, H. H. Zhang⁵⁴, H. Y. Zhang^{1,53}, J. J. Zhang⁴⁷, J. L. Zhang⁷², J. Q. Zhang³⁷, J. W. Zhang^{1,53,58}, J. X. Zhang^{34,j,k}, J. Y. Zhang¹, J. Z. Zhang^{1,58}, Jianyu Zhang^{1,58}, Jiawei Zhang^{1,58}, L. M. Zhang⁵⁶, L. Q. Zhang⁵⁴, Lei Zhang³⁸, P. Zhang¹, Q. Y. Zhang^{35,75}, Shuihan Zhang^{1,58}, Shulei Zhang^{23,h}, X. D. Zhang⁴¹, X. M. Zhang¹, X. Y. Zhang⁵⁰, X. Y. Zhang⁴⁵, Y. Zhang⁶⁴, Y. T. Zhang⁷⁵, Y. H. Zhang^{1,53}, Yan Zhang^{66,53}, Yao Zhang¹, Z. H. Zhang¹, Z. Y. Zhang⁷¹, Z. Y. Zhang³⁹, G. Zhao¹, J. Zhao³⁵, J. Y. Zhao^{1,58}, J. Z. Zhao^{1,53}, Lei Zhao^{66,53}, Ling Zhao¹, M. G. Zhao³⁹, Q. Zhao¹, S. J. Zhao⁷⁵, Y. B. Zhao^{1,53}, Y. X. Zhao^{28,58}, Z. G. Zhao^{66,53}, A. Zhemchugov^{32,a}, B. Zheng⁶⁷, J. P. Zheng^{1,53}, Y. H. Zheng⁵⁸, B. Zhong³⁷, C. Zhong⁶⁷, X. Zhong⁵⁴, H. Zhou⁴⁵, L. P. Zhou^{1,58}, X. Zhou⁷¹, X. K. Zhou⁵⁸, X. R. Zhou^{66,53}, X. Y. Zhou³⁵, Y. Z. Zhou^{10,f}, J. Zhu³⁹, K. Zhu¹, K. J. Zhu^{1,53,58}, L. X. Zhu⁵⁸, S. H. Zhu⁶⁵, S. Q. Zhu³⁸, W. J. Zhu^{10,f}, Y. C. Zhu^{66,53}, Z. A. Zhu^{1,58}, B. S. Zou¹, J. H. Zou¹, J. Zu^{66,53}

(BESIII Collaboration)

- ¹ Institute of High Energy Physics, Beijing 100049, People's Republic of China
² Beihang University, Beijing 100191, People's Republic of China
³ Beijing Institute of Petrochemical Technology, Beijing 102617, People's Republic of China
⁴ Bochum Ruhr-University, D-44780 Bochum, Germany
⁵ Carnegie Mellon University, Pittsburgh, Pennsylvania 15213, USA
⁶ Central China Normal University, Wuhan 430079, People's Republic of China
⁷ Central South University, Changsha 410083, People's Republic of China
⁸ China Center of Advanced Science and Technology, Beijing 100190, People's Republic of China
⁹ COMSATS University Islamabad, Lahore Campus, Defence Road, Off Raiwind Road, 54000 Lahore, Pakistan
¹⁰ Fudan University, Shanghai 200433, People's Republic of China
¹¹ G.I. Budker Institute of Nuclear Physics SB RAS (BINP), Novosibirsk 630090, Russia
¹² GSI Helmholtzcentre for Heavy Ion Research GmbH, D-64291 Darmstadt, Germany
¹³ Guangxi Normal University, Guilin 541004, People's Republic of China
¹⁴ Guangxi University, Nanning 530004, People's Republic of China
¹⁵ Hangzhou Normal University, Hangzhou 310036, People's Republic of China
¹⁶ Hebei University, Baoding 071002, People's Republic of China
¹⁷ Helmholtz Institute Mainz, Staudinger Weg 18, D-55099 Mainz, Germany
¹⁸ Henan Normal University, Xinxiang 453007, People's Republic of China
¹⁹ Henan University of Science and Technology, Luoyang 471003, People's Republic of China
²⁰ Henan University of Technology, Zhengzhou 450001, People's Republic of China
²¹ Huangshan College, Huangshan 245000, People's Republic of China
²² Hunan Normal University, Changsha 410081, People's Republic of China
²³ Hunan University, Changsha 410082, People's Republic of China
²⁴ Indian Institute of Technology Madras, Chennai 600036, India
²⁵ Indiana University, Bloomington, Indiana 47405, USA
²⁶ INFN Laboratori Nazionali di Frascati, (A)INFN Laboratori Nazionali di Frascati, I-00044, Frascati, Italy; (B)INFN Sezione di Perugia, I-06100, Perugia, Italy; (C)University of Perugia, I-06100, Perugia, Italy
²⁷ INFN Sezione di Ferrara, (A)INFN Sezione di Ferrara, I-44122, Ferrara, Italy; (B)University of Ferrara, I-44122, Ferrara, Italy
²⁸ Institute of Modern Physics, Lanzhou 730000, People's Republic of China
²⁹ Institute of Physics and Technology, Peace Avenue 54B, Ulaanbaatar 13330, Mongolia
³⁰ Jilin University, Changchun 130012, People's Republic of China
³¹ Johannes Gutenberg University of Mainz, Johann-Joachim-Becher-Weg 45, D-55099 Mainz, Germany
³² Joint Institute for Nuclear Research, 141980 Dubna, Moscow region, Russia
³³ Justus-Liebig-Universitaet Giessen, II. Physikalisches Institut, Heinrich-Buff-Ring 16, D-35392 Giessen, Germany
³⁴ Lanzhou University, Lanzhou 730000, People's Republic of China

- ³⁵ Liaoning Normal University, Dalian 116029, People's Republic of China
- ³⁶ Liaoning University, Shenyang 110036, People's Republic of China
- ³⁷ Nanjing Normal University, Nanjing 210023, People's Republic of China
- ³⁸ Nanjing University, Nanjing 210093, People's Republic of China
- ³⁹ Nankai University, Tianjin 300071, People's Republic of China
- ⁴⁰ National Centre for Nuclear Research, Warsaw 02-093, Poland
- ⁴¹ North China Electric Power University, Beijing 102206, People's Republic of China
- ⁴² Peking University, Beijing 100871, People's Republic of China
- ⁴³ Qufu Normal University, Qufu 273165, People's Republic of China
- ⁴⁴ Shandong Normal University, Jinan 250014, People's Republic of China
- ⁴⁵ Shandong University, Jinan 250100, People's Republic of China
- ⁴⁶ Shanghai Jiao Tong University, Shanghai 200240, People's Republic of China
- ⁴⁷ Shanxi Normal University, Linfen 041004, People's Republic of China
- ⁴⁸ Shanxi University, Taiyuan 030006, People's Republic of China
- ⁴⁹ Sichuan University, Chengdu 610064, People's Republic of China
- ⁵⁰ Soochow University, Suzhou 215006, People's Republic of China
- ⁵¹ South China Normal University, Guangzhou 510006, People's Republic of China
- ⁵² Southeast University, Nanjing 211100, People's Republic of China
- ⁵³ State Key Laboratory of Particle Detection and Electronics, Beijing 100049, Hefei 230026, People's Republic of China
- ⁵⁴ Sun Yat-Sen University, Guangzhou 510275, People's Republic of China
- ⁵⁵ Suranaree University of Technology, University Avenue 111, Nakhon Ratchasima 30000, Thailand
- ⁵⁶ Tsinghua University, Beijing 100084, People's Republic of China
- ⁵⁷ Turkish Accelerator Center Particle Factory Group, (A)Istinye University, 34010, Istanbul, Turkey; (B)Near East University, Nicosia, North Cyprus, Mersin 10, Turkey
- ⁵⁸ University of Chinese Academy of Sciences, Beijing 100049, People's Republic of China
- ⁵⁹ University of Groningen, NL-9747 AA Groningen, The Netherlands
- ⁶⁰ University of Hawaii, Honolulu, Hawaii 96822, USA
- ⁶¹ University of Jinan, Jinan 250022, People's Republic of China
- ⁶² University of Manchester, Oxford Road, Manchester, M13 9PL, United Kingdom
- ⁶³ University of Muenster, Wilhelm-Klemm-Strasse 9, 48149 Muenster, Germany
- ⁶⁴ University of Oxford, Keble Road, Oxford OX13RH, United Kingdom
- ⁶⁵ University of Science and Technology Liaoning, Anshan 114051, People's Republic of China
- ⁶⁶ University of Science and Technology of China, Hefei 230026, People's Republic of China
- ⁶⁷ University of South China, Hengyang 421001, People's Republic of China
- ⁶⁸ University of the Punjab, Lahore-54590, Pakistan
- ⁶⁹ University of Turin and INFN, (A)University of Turin, I-10125, Turin, Italy; (B)University of Eastern Piedmont, I-15121, Alessandria, Italy; (C)INFN, I-10125, Turin, Italy
- ⁷⁰ Uppsala University, Box 516, SE-75120 Uppsala, Sweden
- ⁷¹ Wuhan University, Wuhan 430072, People's Republic of China
- ⁷² Xinyang Normal University, Xinyang 464000, People's Republic of China
- ⁷³ Yunnan University, Kunming 650500, People's Republic of China
- ⁷⁴ Zhejiang University, Hangzhou 310027, People's Republic of China
- ⁷⁵ Zhengzhou University, Zhengzhou 450001, People's Republic of China
- ^a Also at the Moscow Institute of Physics and Technology, Moscow 141700, Russia
- ^b Also at the Novosibirsk State University, Novosibirsk, 630090, Russia
- ^c Also at the NRC "Kurchatov Institute", PNPI, 188300, Gatchina, Russia
- ^d Also at Goethe University Frankfurt, 60323 Frankfurt am Main, Germany
- ^e Also at Key Laboratory for Particle Physics, Astrophysics and Cosmology, Ministry of Education; Shanghai Key Laboratory for Particle Physics and Cosmology; Institute of Nuclear and Particle Physics, Shanghai 200240, People's Republic of China
- ^f Also at Key Laboratory of Nuclear Physics and Ion-beam Application (MOE) and Institute of Modern Physics, Fudan University, Shanghai 200443, People's Republic of China
- ^g Also at State Key Laboratory of Nuclear Physics and Technology, Peking University, Beijing 100871, People's Republic of China
- ^h Also at School of Physics and Electronics, Hunan University, Changsha 410082, China
- ⁱ Also at Guangdong Provincial Key Laboratory of Nuclear Science, Institute of Quantum Matter, South China Normal University, Guangzhou 510006, China
- ^j Also at Frontiers Science Center for Rare Isotopes, Lanzhou University, Lanzhou 730000, People's Republic of China

Abstract

We report a search for a dark photon using 14.9 fb^{-1} of e^+e^- annihilation data taken at center-of-mass energies from 4.13 to 4.60 GeV with the BESIII detector operated at the BEPCII storage ring. The dark photon is assumed to be produced in the initial state radiation process and to predominantly decay into light dark matter particles, which escape from the detector undetected. The mass range from 1.5 to 2.9 GeV/ c^2 is scanned for the dark photon candidate, and no significant signal is observed. The mass dependent upper limits at the 90% confidence level on the coupling strength parameter ϵ for a dark photon coupling with an ordinary photon vary between 1.6×10^{-3} and 5.7×10^{-3} .

Keywords: dark sector, dark photon, invisible decays

1. Introduction

The Standard Model (SM) of particle physics is powerful but does not address several important phenomena that hint there is physics beyond the SM. One that is not included in the SM is the existence of dark matter (DM), which makes up $\sim 84\%$ of the matter in the universe [1, 2]. DM interactions with ordinary matter are observed through the gravitational effects DM has on galaxies, but the lack of interaction between DM and SM particles via strong, weak, and electromagnetic forces makes it very challenging to detect directly in particle physics experiments. However, recent results from astrophysical observations [3–5], as well as the long-standing discrepancy between the experimental value and the theoretical prediction of the muon anomalous magnetic moment [6, 7] indicate there could be a new force between the dark sector and the SM. The new force could be mediated by a $U(1)_D$ gauge boson γ' (referred to as a dark photon), which couples weakly to a SM photon through kinetic mixing ($\frac{1}{2}\epsilon F'_{\mu\nu}F^{\mu\nu}$) [8–11], where $F'_{\mu\nu}$ and $F_{\mu\nu}$ are the field strengths of the dark photon and the SM photon, respectively, and the mixing parameter ϵ gives the coupling strength between the dark photon and SM photon.

A dark photon with mass in the GeV range and ϵ value as high as $\epsilon \sim 10^{-3}$ has been predicted in Refs. [8, 12, 13]. The small value of epsilon and a suppression factor of ϵ^2 of the coupling between the dark photon and the SM photon make it very hard to detect. However, benefiting from high intensity facilities such as e^+e^- colliders, a dark photon candidate could be produced in particle physics experiments. The dark photon would predominately decay into a pair of DM particles

($\gamma' \rightarrow \chi\bar{\chi}$), which are the lightest DM particles (χ) with masses $m_\chi < m_{\gamma'}/2$, and thus be invisible. Previous measurements on the invisible γ' decays have been performed by the NA62 [14], NA64 [15, 16], BaBar [17], E787 [18] and E949 [19] experiments. No evidence is found for a dark photon, and upper limits for ϵ have been set.

A dark photon can also be searched for at the BESIII experiment via Initial-State-Radiation (ISR) production ($e^+e^- \rightarrow \gamma_{\text{ISR}}\gamma'$), where γ_{ISR} is an ISR photon. The dark photon candidate of mass $m_{\gamma'}$ would be signified by the presence of a monochromatic ISR photon with energy

$$E_{\text{ISR}} = \frac{s - m_{\gamma'}^2 c^4}{2\sqrt{s}}, \quad (1)$$

where \sqrt{s} is the e^+e^- center-of-mass (c.m.) energy.

In this letter, we perform a measurement of the process $e^+e^- \rightarrow \gamma_{\text{ISR}}\gamma'$ at the BESIII experiment located at the Beijing Electron Positron Collider (BEPCII) [20], where the dark photon decays invisibly into a dark matter $\chi\bar{\chi}$ pair. Therefore, the signal process only contains monochromatic single ISR photon events. We reconstruct the dark photon signal by seeking a narrow peak in the ISR photon energy (E_{ISR}) spectrum, which is related to the missing mass $m_{\gamma'}$ of the recoil system through Eq. (1). The analysis is based on the data sets taken at $\sqrt{s} = 4.13$ to 4.60 GeV, corresponding to an integrated luminosity of 14.9 fb^{-1} [21].

2. Detector and Monte Carlo simulation

The BESIII detector [22] records symmetric e^+e^- collisions provided by the BEPCII storage ring [20],

which operates with a peak luminosity of $1 \times 10^{33} \text{ cm}^{-2}\text{s}^{-1}$ in the center-of-mass energy range from 2.0 to 4.95 GeV. BESIII has collected large data samples in this energy region [23]. The cylindrical core of the BESIII detector covers 93% of the full solid angle and consists of a helium-based multilayer drift chamber (MDC), a plastic scintillator time-of-flight system (TOF), and a CsI(Tl) electromagnetic calorimeter (EMC), which are all enclosed in a superconducting solenoidal magnet providing a 1.0 T magnetic field. The solenoid is supported by an octagonal flux-return yoke with 9 layers of resistive plate counters interleaved with steel, comprising a muon identification system (MUC). The charged-particle momentum resolution at 1 GeV/c is 0.5%, and the specific energy loss (dE/dx) resolution is 6% for electrons from Bhabha scattering. The EMC measures photon energies with a resolution of 2.5% (5%) at 1 GeV in the barrel (end cap) region. The time resolution in the TOF barrel region is 68 ps, while that in the end cap region is 110 ps. The end cap TOF system was upgraded in 2015 using multigap resistive plate chamber technology, providing a time resolution of 60 ps [24]. The spatial resolution in the MUC is better than 2 cm.

Simulated Monte Carlo (MC) samples produced with GEANT4-based [25] software, including the geometrical description of the BESIII detector and the detector response, are used to determine the detection efficiency, and to estimate potential backgrounds. The signal MC events for the reaction $e^+e^- \rightarrow \gamma_{\text{ISR}}\gamma'$ are generated using EVTGEN [26] for 29 different γ' mass hypotheses in the range from 1.5 to 2.9 GeV with a 50 MeV step size. The dominant background source comes from the di-gamma process ($e^+e^- \rightarrow \gamma\gamma$), which is generated using the BABAYAGANLO generator [27]. The other possible background sources are investigated with inclusive MC simulation samples, consisting of open-charm processes, the ISR production of lower mass vector charmonium(-like) states, and the continuum processes. The known decay modes of charmed hadrons are handled by EVTGEN [26] with known decay branching fractions taken from the Particle Data Group (PDG) [28] and the remaining unknown decays with LUNDCHARM [29].

3. Event selection

The signal events have only one monochromatic photon. Thus, events with any reconstructed charged tracks in the MDC are rejected. Photon candidates are required to have deposited energy larger than 25 MeV in the barrel EMC region ($|\cos\theta| < 0.8$) or larger than

50 MeV in the end cap region ($0.86 < |\cos\theta| < 0.92$), where θ is the polar angle of each photon candidate. To remove contamination from fake photons, the number of photons (N_γ) in each event should satisfy $1 \leq N_\gamma \leq 3$. The most energetic photon is regarded as the candidate for the signal photon (γ_{ISR}). To suppress the overwhelming di-gamma background events, the polar angle of the signal photon is required to be within $|\cos\theta| < 0.6$. As our signal events are purely neutral events, the event start time t_0 is determined from hits in TOF when available or otherwise the trigger time by the EMC. To suppress electronic noise and energy deposition unrelated to the physical events, the EMC time of γ_{ISR} is required to be within [-500, 1250] ns with respect to t_0 , where the values are obtained by studying a di-gamma control sample.

Backgrounds with multiple photons in the final state, such as $e^+e^- \rightarrow \gamma\gamma, \gamma\gamma\gamma$, etc., can be effectively suppressed by requiring the total deposited energy of showers except for γ_{ISR} (denoted as E_{extra}) in the EMC be less than 80 MeV. To eliminate the backgrounds from neutral hadrons, such as $e^+e^- \rightarrow n\bar{n}$, which also produce showers in the EMC, two shower shape related variables, the lateral moment and energy ratio in 3×3 and 5×5 crystals around the central seed crystal (E_9/E_{25}), are used to distinguish showers caused by neutral hadrons from photons. The lateral moment is given by

$$\frac{\sum_{i=3}^n E_i r_i^2}{\sum_{i=3}^n E_i r_i^2 + E_1 r_0^2 + E_2 r_0^2}, \quad (2)$$

where n is the number of crystals associated with the shower, E_i is the deposited energy in the i th crystal and $E_1 > E_2 > \dots > E_n$, r_i is the lateral distance between the central and the i th crystal, and r_0 is the average distance between the two crystals. A γ_{ISR} candidate is required to have a lateral moment larger than 0.14 and less than 0.3 as well as a value of $E_9/E_{25} > 0.95$.

Due to the structure of the EMC, one of the photons from a di-gamma event can penetrate the calorimeter in the gap between the barrel and the endcap ($0.8 < |\cos\theta| < 0.86$), or occasionally pass between crystals in the zenith angle direction ($\cos\theta = 0$), producing a sole photon in the detector, and thereby mimicking a signal event. An escaped energetic photon often interacts in the outer detector material and produces secondary particles, which are then recorded by the MUC. To suppress this background, events with MUC hits within $|\cos\theta_{\text{hit}}| > 0.65$ or $|\cos\theta_{\text{hit}}| < 0.06$, where θ_{hit} is the polar angle of the MUC hit, are rejected.

4. The ISR photon energy spectrum

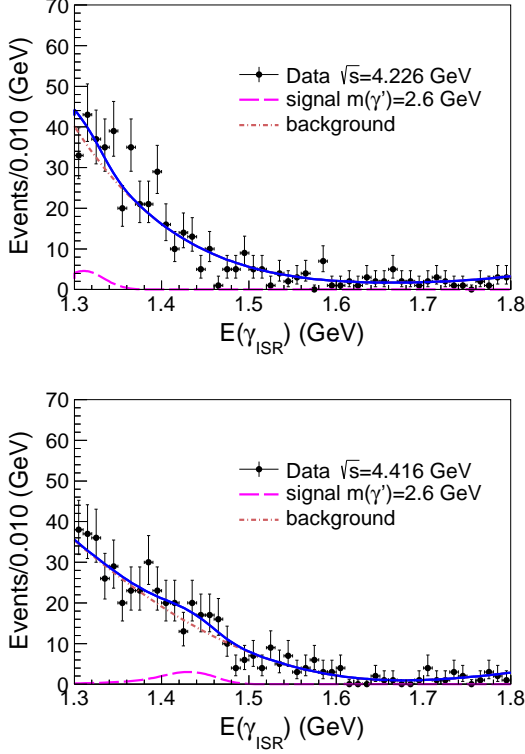


FIG. 1: ISR photon energy spectra at $\sqrt{s} = 4.226$ GeV (top) and $\sqrt{s} = 4.416$ GeV (bottom) with fit projections overlaid. The magenta dashed curves are the dark photon signal shapes with $m_{\gamma'} = 2.6$ GeV/ c^2 , which depend on the c.m. energy of the data set according to Eq. (1). Dots with error bars are data, the blue solid curves are the total fit results, and the red dot-dashed curves describe the background contributions.

After imposing the above event selection criteria, the γ_{ISR} energy spectra at $\sqrt{s} = 4.178$ and 4.226 GeV are shown as examples in Fig. 1. The trigger efficiency for single photons in the barrel EMC is relatively low, and the background from di-gamma events is high for $E(\gamma_{\text{ISR}}) < 1.3$ GeV. In addition, a photon candidate with energy larger than 2 GeV will saturate the EMC electronics, which results in shower loss. Such effects would lead to a significant number of di-gamma background events when one energetic photon candidate is lost. Therefore, we only search for a dark photon signal within the range $1.3 < E(\gamma_{\text{ISR}}) < 1.8$ GeV corresponding to $1.5 < m_{\gamma'} < 2.9$ GeV/ c^2 , according to Eq. (1).

The production cross section for a dark photon can-

didate can be calculated by [10]

$$\sigma(e^+e^- \rightarrow \gamma_{\text{ISR}}\gamma') = \frac{2\pi\alpha^2}{s}\epsilon^2(1-x) \left(\left(1 + \frac{2x}{(1-x)^2}\right)\Theta - 2\cos\theta_c \right), \quad (3)$$

where $x = \frac{m_{\gamma'}^2}{s}$, $\Theta = \log\left(\frac{1+\cos\theta_c}{1-\cos\theta_c}\right)^2$, $\cos\theta_c = 0.6$ is the $\cos\theta$ limit for the ISR photon polar angle, and α is the fine-structure constant. The coupling strength parameter ϵ^2 which determines the cross section is common and shared for all c.m. energy data samples. The expected signal yield at a certain c.m. energy is $N^{\text{sig}} = \mathcal{L}\sigma(e^+e^- \rightarrow \gamma_{\text{ISR}}\gamma')\epsilon_{\text{det}}\epsilon_{\text{trig}}$, where \mathcal{L} is the integrated luminosity of the data [21], ϵ_{det} is the signal detection efficiency and ϵ_{trig} is the trigger efficiency.

The detection efficiencies for signal events at each c.m. energy for specific values of $m_{\gamma'}$ are obtained by simulated signal MC samples, and depending on $m_{\gamma'}$ and the c.m. energy, vary between 1% and 6%. The trigger efficiency for single photon events is studied via radiative Bhabha events ($e^+e^- \rightarrow \gamma e^+e^-$). In order to select a clean radiative Bhabha sample in the EMC barrel region, we require either $e^\pm\gamma$ or e^+e^- be detected by the endcap detector and a third e^\pm or γ hit the barrel EMC. We find $\epsilon_{\text{trig}} = (99.40 \pm 0.01)\%$ for events with $E(\gamma_{\text{ISR}}) > 1.3$ GeV, and the efficiency drops dramatically for $E(\gamma_{\text{ISR}}) < 1.3$ GeV.

To determine the signal yield for each $m_{\gamma'}$ hypothesis, an simultaneous unbinned maximum likelihood fit to the ISR photon energy spectra is performed to all data sets. The signal yields for each data set depend on the common parameter ϵ , according to Eq.(3). In the fit, the signal shape for each c.m. energy is modeled by a corresponding signal MC shape convolved with a Gaussian function, which represents the photon energy resolution difference between data and MC simulation. The parameters of the Gaussian function are determined by a di-gamma control sample. The background shape for each c.m. energy is described by a 4th order polynomial function. To obtain the signal yield for different $m_{\gamma'}$ candidates, we scan the $m_{\gamma'}$ region with a 50 MeV/ c^2 step size (in total 29 steps) and repeat the fit. Figure 1 shows the fit results for a dark photon candidate with $m_{\gamma'} = 2.6$ GeV at $\sqrt{s} = 4.26$ and 4.416 GeV. After taking into account the uncertainty from the background model, the maximum local significance is determined to be 3.1σ at $m_{\gamma'} = 2.6$ GeV. The statistical significances are calculated by comparing the likelihoods with and without the signal components in the fit, and taking the change of the number of

degrees of freedom into account. Figure 2 shows the estimated local statistical significance for different $m_{\gamma'}$ hypotheses. The maximum global significance, taking the Look-Elsewhere Effect [30] into account, is determined to be 2.2σ . Therefore, a null result is reported for the search of a dark photon with invisible decays.

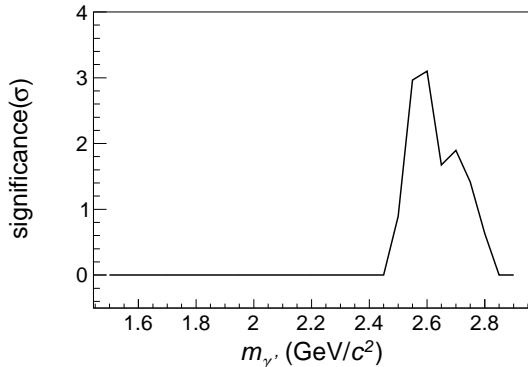


FIG. 2: Local statistical significance for dark photon candidates obtained from the fit to the photon energy spectrum as a function of $m_{\gamma'}$.

5. Upper limit for coupling strength

Since no significant dark photon signal is observed, we set an upper limit on ϵ at the 90% confidence level (C.L.). From Eq. 3, for a given dark photon mass, the expected signal event yield in data depends on ϵ . Applying a Bayesian method, a likelihood scan is performed by varying the value of ϵ in the simultaneous fit to all data sets,

$$\int_0^{\epsilon_{90\%}} \mathcal{L}(\epsilon) d\epsilon = 90\% \int_0^{\infty} \mathcal{L}(\epsilon) d\epsilon \quad (4)$$

where $\mathcal{L}(\epsilon)$ is the ϵ -dependent likelihood value, and $\epsilon_{90\%}$ represents the coupling strength parameter which corresponds to 90% of the integral of the likelihood function from $\epsilon = 0$ to ∞ . To consider the systematic uncertainty, the likelihood curves are also convolved with a Gaussian function with its standard deviation set to the value of the systematic uncertainty. The upper limits of ϵ at the 90% C.L. versus the dark photon mass are shown in Fig. 3, and $\epsilon_{90\%}$ varies within $(1.6 - 5.7) \times 10^{-3}$, depending on $m_{\gamma'}$ between 1.5 and 2.9 GeV/ c^2 .

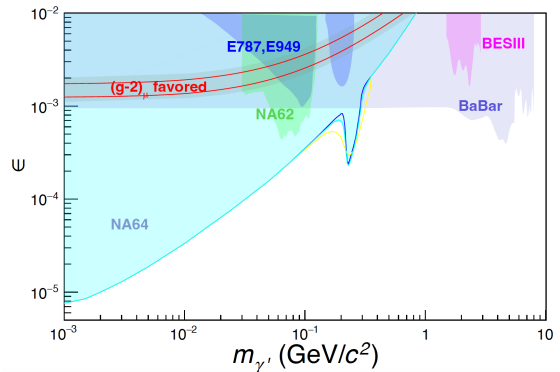


FIG. 3: Upper limit on the coupling strength (ϵ) between the dark sector and the SM at the 90% C.L. versus the dark photon mass measured by BESIII (magenta region), together with previous measurements [14–19], as well as the parameter region favored by the $(g-2)_\mu$ anomaly [31]. The two red lines correspond to $(g-2)_\mu + 2\sigma$ and $(g-2)_\mu - 2\sigma$ and take into account the latest result from Fermilab [7].

6. Systematic uncertainties

The systematic uncertainties for the ϵ measurement include those from the luminosity measurement, photon detection efficiency, selection criteria, photon resolution, and determination of the trigger efficiency. The luminosity of the data sets used is measured using large angle Bhabha scattering events, with an uncertainty less than 1.0% [21]. The signal process has only one signal photon, and 1.0% is assigned as the uncertainty from the photon detection efficiency [32].

The systematic uncertainties from the requirement on the number of photons, EMC time, E_{extra} , EMC shower shapes, and MUC hits are investigated with a clean di-gamma control sample. We use two back-to-back photons with energies close to the beam energy to select a di-gamma control sample from the same data sets [21]. The systematic uncertainties, which are determined from the differences between signal MC events and di-gamma data events, are 1.4% for the number of photons, 1.4% for the EMC time, 0.3% for E_{extra} , 0.4% for EMC shower shapes, and 8.5% for the MUC hits.

In our fits to the photon energy spectra, the signal shape is convolved with a Gaussian function to account for the resolution difference between data and MC simulation. The parameters of the Gaussian function are obtained from di-gamma data events with c.m. energies from 2.644 to 3.400 GeV to ensure the photon energy is similar to the signal process. To determine the systematic uncertainty due to both the photon energy resolution and background modeling, the fit is repeated with alternative signal and background shapes, i.e. varying the width of the Gaussian function used to convolve the

signal shape according to its uncertainty, and using the $(n+1)^{th}$ order polynomial functions for the background shape. The one with the largest upper limit value for ϵ is taken as the final result.

For the systematic uncertainty due to the trigger efficiency, the small trigger efficiency difference measured by electrons and photons in the EMC barrel, which is 1.0%, is taken as the systematic uncertainty.

Table 1 lists all considered sources of systematic uncertainties. Assuming they are independent, the total systematic uncertainty is the sum in quadrature of the individual contributions and is determined to be 8.9%.

TABLE 1: Sources of relative systematic uncertainties and their contributions (%).

Source	Uncertainty (%)
Luminosity	1.0
Photon detection	1.0
Number of photons	1.4
EMC time	1.4
E_{extra}	0.3
Shower shapes	0.4
MUC hits	8.5
Trigger efficiency	1.0
Total	8.9

7. Summary

In summary, using data collected by the BESIII experiment at c.m. energies from 4.13 to 4.60 GeV corresponding to an integrated luminosity of 14.9 fb^{-1} , we search for the Initial State Radiation production of a dark photon which decays invisibly. No obvious signal is observed in the mass region between 1.5 and 2.9 GeV/c^2 , and the upper limit on the coupling strength parameter ϵ at the 90% C.L. is determined to be within $(1.6 - 5.7) \times 10^{-3}$ as a function of the dark photon mass. Our exclusion limits are below the $(g-2)_\mu$ anomaly values in our mass region but are somewhat higher than the previous measurement from the BaBar experiment [17].

The BESIII collaboration thanks the staff of BEPCII and the IHEP computing center for their strong support. This work is supported in part by National Key R&D Program of China under Contracts Nos. 2020YFA0406400, 2020YFA0406300; National Natural Science Foundation of China (NSFC) under Contracts Nos. 11635010, 11735014, 11835012, 11935015, 11935016, 11935018, 11961141012, 12022510, 12025502, 12035009, 12035013, 12192260, 12192261, 12192262, 12192263, 12192264, 12192265; the Chinese Academy of Sciences (CAS) Large-Scale Scientific Facility Program; Joint Large-Scale Scientific Facility Funds of the NSFC and CAS under Contract No. U1832207; CAS Key Research Program of Frontier Sciences under Contract No. QYZDJ-SSW-SLH040; 100 Talents Program of CAS; INPAC and Shanghai Key Laboratory for Particle Physics and Cosmology; ERC under Contract No. 758462; European Union's Horizon 2020 research and innovation programme under Marie Skłodowska-Curie grant agreement under Contract No. 894790; German Research Foundation DFG under Contracts Nos. 443159800, Collaborative Research Center CRC 1044, GRK 2149; Istituto Nazionale di Fisica Nucleare, Italy; Ministry of Development of Turkey under Contract No. DPT2006K-120470; National Science and Technology fund; STFC (United Kingdom); The Royal Society, UK under Contracts Nos. DH140054, DH160214; The Swedish Research Council; U. S. Department of Energy under Contract No. DE-FG02-05ER41374.

tic Facility Program; Joint Large-Scale Scientific Facility Funds of the NSFC and CAS under Contract No. U1832207; CAS Key Research Program of Frontier Sciences under Contract No. QYZDJ-SSW-SLH040; 100 Talents Program of CAS; INPAC and Shanghai Key Laboratory for Particle Physics and Cosmology; ERC under Contract No. 758462; European Union's Horizon 2020 research and innovation programme under Marie Skłodowska-Curie grant agreement under Contract No. 894790; German Research Foundation DFG under Contracts Nos. 443159800, Collaborative Research Center CRC 1044, GRK 2149; Istituto Nazionale di Fisica Nucleare, Italy; Ministry of Development of Turkey under Contract No. DPT2006K-120470; National Science and Technology fund; STFC (United Kingdom); The Royal Society, UK under Contracts Nos. DH140054, DH160214; The Swedish Research Council; U. S. Department of Energy under Contract No. DE-FG02-05ER41374.

References

- [1] N. Aghanim *et al.* (Planck), *Planck 2018 results. VI. Cosmological parameters*, *Astron. J.*
- [2] G. Bertone and D. Hooper, *History of dark matter*, *Rev. Mod. Phys.* **90**, 045002 (2018).
- [3] O. Adriani *et al.* (PAMELA), *An anomalous positron abundance in cosmic rays with*
- [4] M. Ackermann *et al.* (Fermi-LAT), *Measurement of separate cosmic-ray electron and*
- [5] M. Aguilar *et al.* (AMS), *First Result from the Alpha Magnetic Spectrometer on the*
- [6] G. W. Bennett *et al.* (Muon g-2), *Final Report of the Muon E821 Anomalous Magnetic*
- [7] B. Abi *et al.* (Muon g-2), *Measurement of the Positive Muon Anomalous Magnetic*
- [8] R. Essig, J. A. Jaros, W. Wester, P. Hansson Adrian, S. Andreas, T. Averett, O. Baker
- [9] N. Arkani-Hamed, D. P. Finkbeiner, T. R. Slatyer and N. Weiner, *A Theory of Dark*
- [10] R. Essig, P. Schuster and N. Toro, *Probing Dark Forces and Light Hidden Sectors at*
- [11] S. Andreas, C. Niebuhr and A. Ringwald, *New Limits on Hidden Photons from Past*
- [12] N. Arkani-Hamed and N. Weiner, *LHC Signals for a SuperUnified Theory of Dark M*
- [13] M. Pospelov, A. Ritz and M. B. Voloshin, *Secluded WIMP Dark Matter*, *Phys. Lett.*
- [14] E. Cortina Gil *et al.* (NA62), *Search for production of an invisible dark photon in π^0*
- [15] D. Banerjee *et al.* (NA64), *Search for invisible decays of sub-GeV dark photons in n*
- [16] Y. M. Andreev, D. Banerjee, J. Bernhard, M. Bondi, V. E. Burtsev, A. Celentano, N.
- [17] J. P. Lees *et al.* (BaBar), *Search for Invisible Decays of a Dark Photon Produced in*
- [18] S. Adler *et al.* (E787), *Further evidence for the decay $K^+ \rightarrow \pi^+ \nu \bar{\nu}$* , *Phys. Rev. Lett.*
- [19] A. V. Artamonov *et al.* (BNL-E949), *Study of the decay $K^+ \rightarrow \pi^+ \nu \bar{\nu}$ in the momen*
- [20] C. H. Yu *et al.*, *BEPCII Performance and Beam Dynamics Studies on Luminosity*, in
- [21] M. Ablikim *et al.* (BESIII), *Measurement of the integrated luminosities at BESIII for*
- [22] M. Ablikim *et al.* (BESIII), *Design and Construction of the BESIII Detector*, *Nucl. I*
- [23] M. Ablikim *et al.* (BESIII), *Future Physics Programme of BESIII*, *Chin. Phys. C* **44**
- [24] X. Li *et al.*, *Study of MRPC technology for BESIII endcap-TOF upgrade*, *Radiat. De*
- [25] Y. X. Guo *et al.*, *The study of time calibration for upgraded end cap TOF of BESIII*, in
- [26] P. Cao *et al.*, *Design and construction of the new BESIII endcap Time-of-Flight syst*
- [27] S. Agostinelli *et al.* (GEANT4), *Geant4Na simulation toolkit*, *Nucl. Instrum. Method*
- [28] D. J. Lange, *The EvtGen particle decay simulation package*, *Nucl. Instrum. Method*
- [29] R. G. Ping, *Event generators at BESIII*, *Chin. Phys. C* **32**, 599 (2008).
- [30] G. Balossini, C. M. Carloni Calame, G. Montagna, O. Nicrosini and F. Piccinini, *M*
- [31] P. A. Zyla *et al.* (Particle Data Group), *Review of Particle Physics*, *Prog. Theor. Exp*
- [32] J. C. Chen, G. S. Huang, X. R. Qi, D. H. Zhang and Y. S. Zhu, *Event generator for a*
- [33] R. L. Yang, R. G. Ping and H. Chen, *Tuning and Validation of the Lundcharm Mode*
- [34] J. P. Lees *et al.* (BaBar), *Search for di-muon decays of a low-mass Higgs boson in r*
- [35] P. Fayet, *U-boson production in $e^+ e^-$ annihilations, ψ and Upsilon decays, and L*
- [36] M. Ablikim *et al.* (BESIII), *Branching fraction measurements of χ_{c0} and χ_{c2} to π^0*